

An Optimization-based Approach to Fusion of Multi-Exposure, Low Dynamic Range Images

Ketan Kotwal and Subhasis Chaudhuri
Electrical Engineering Department
Indian Institute of Technology Bombay
Mumbai, India
Email: {ketan, sc}@ee.iitb.ac.in

Abstract—The problem of compositing a high dynamic range (HDR) image for display on a standard low dynamic range device involves matte-based fusion of multiple images captured with different camera exposures, followed by a suitable tone mapping of the fused HDR image. The fused image should represent the entire scene in a clear, well-exposed manner by bringing the under- and over-exposed regions from the input images into the display range of the device while preserving the local contrast. We define matting as a multi-objective optimization problem based on these desired characteristics of the output, and provide the solution using an Euler-Lagrange technique. The proposed technique yields visually appealing fused images with a high value of contrast. Our technique produces the fused image of a low dynamic range, and thus it eliminates the need for generation of an intermediate HDR image and associated tone mapping. Additionally, our technique does not require any knowledge of the camera response functions or exposure settings.

Keywords: Image fusion, high dynamic range imaging, unconstrained optimization, Euler-Lagrange method.

I. INTRODUCTION

We frequently encounter with the real world scenes having a very high dynamic range. The irradiance varies greatly over the scene, which most of the digital camera systems are not capable of capturing due to their low dynamic range. For example, in many of the imaging devices this range is limited to 8 bits per color plane, and thus, these devices impose a severe shortcoming in faithful acquisition of the scene. In such images, several regions either appear very dark or over-exposed. Most of the computer vision algorithms rely on a robust and precise capture of the scene. The low dynamic range images are difficult to process by computer vision algorithms due to lack of either illumination or poor details due to saturation. A frequently observed example is night time images, which are difficult to process due to poorly captured information especially in the background. A common low cost solution to this problem of obtaining high dynamic range (HDR) scenes is to capture multiple images of the same scene by varying the exposure time of the fixed camera. This set of low dynamic range (LDR) images as a whole, captures the entire range of the scene, as every LDR image represents in detail some parts of the scene depending on the exposure settings. A long exposure time of the camera facilitates capturing details in the dark scene regions, whereas an LDR image captured with a short exposure time provides details in the very bright scene areas. Each of the LDR images

provides a well exposed capture of some part of the scene. These multiple LDR images are suitably fused to generate a single HDR image with an enhanced quality. This fused image provides a better visualization of the scene, and improves the performance of the vision algorithms to be applied thereafter.

The displaying devices, however, have a limited dynamic range, and therefore the HDR image has to be converted into an LDR image using some tone mapping operator [1]. The objective of the tone mapping process is to compress the large intensity range of the image while preserving a local contrast in the image, i.e., to create an “HDR-like” image of a low dynamic range (say, 8-bit).

Most of the early techniques for the multi-exposure fusion make explicit use of camera parameters like camera response function [1], shutter speed [2], [3], etc. These techniques require either the knowledge or estimation of the camera parameters which is not always available, and therefore, the interest lies in obtaining the solution of an HDR problem without this information. The pixels in the set of multiple low dynamic range (LDR) images are appropriately fused to generate an output image which would appear as a high dynamic range (HDR) image seen on the low range display after suitable tone mapping [3]. A variety of tone mapping operators have been suggested for efficient re-mapping of the intensity such as logarithmic mapping [4], gradient domain mapping [5], multi-resolution pyramid based mapping [6], etc.

Recent techniques of multi-exposure fusion eliminate an intermediate step of tone mapping, and produce an HDR-like image directly from the fusion of a set of multi-exposure LDR images. Goshtasby [7] proposed a fusion based on partitioning of the input LDR images into sub blocks and then the sub block with the maximum information content across all the set of images is selected. These blocks are merged together using a normalized blending function. A matte-based technique for the fusion of images captured at variable exposure time is proposed in [8]. This technique uses an edge preserving bilateral filter for the creation of a matte, and then generates the fused image from the normalized matte functions. A matte-less solution to the problem of HDR imaging based on unconstrained optimization is developed in [9]. Mertens *et al.* proposed a multi-resolution based exposure fusion technique which generates the resultant image with the help of certain quality measures like saturation, contrast and well-exposedness [10].

Gallo *et al.* [11] proposed a technique for the generation of a fused image free from ghosting artifacts which is capable of handling input images containing movement. In all these methods, the fusion strategy is quite ad hoc in nature. A Bayesian framework based maximum likelihood solution to the fusion of multi-exposure images with motion blur in the input LDR images is proposed in [12]. To overcome the problem of blurry and noisy input images, Tico *et al.* [13] suggested a two step fusion algorithm that consists of fusion of a photometrically modified LDR image of shortest exposure time with an HDR image generated using the exposure fusion technique described in [10].

In most of the existing work, the fusion of multiple images is obtained via a linear combination of the pixels using a set of predefined rules. These rules usually estimate the “quality” of the particular pixel, and accordingly define the weight factor for the same. These rules are, thus, ad hoc in nature as they do not consider any properties of the input data or how the fused image should appear. In this paper, we define the problem of multi-exposure fusion in an optimization framework, but unlike in [9], the proposed solution is matte-based and the optimization method attempts to estimate the best possible matte for fusion purposes. Based on the desired characteristics of the fused image, we develop a multi-objective cost function, and provide an iterative solution using the variational method. Therefore, the fusion rules in our case are adaptively derived from the data and the corresponding fused image at every iteration. The proposed solution is purely defined on the image qualities, and it does not involve knowledge or estimation of any of the parameters of the imaging system which makes it generic and computationally simpler. The proposed approach fuses multiple LDR images into a single LDR image, but with the quality of an HDR image, and eliminates generation of any intermediate HDR image and tone mapping process.

II. PROPOSED APPROACH

First, we discuss some of the objectives based upon the quality measures of a fused image, and derive the corresponding optimization function. Subsequently we provide a solution to the problem using the Euler-Lagrange method.

A. Formulation of Objective Function

The basic approach for pixel-based fusion is to use a linear combination of pixels across the input images. The final fused image is generated as a normalized weighted sum of the pixels at the given location. Different strategies for the calculation of the weights (popularly known as α -mattes) result in different fusion schemes.

Let \mathbf{U} be the set of N LDR images each with dimensions $(X \times Y)$. We can think of \mathbf{U} as a 3-D array of dimensions $(X \times Y \times N)$ where the individual LDR images are stacked. Let $v(x, y)$ be the fused image of dimensions $(X \times Y)$ generated by an appropriate linear combination of all observations at every pixel location given as-

$$v(x, y) = \sum_{i=1}^N \alpha_i(x, y) u_i(x, y), \quad (1)$$

where $u_i(x, y)$ represents the pixel at location (x, y) in the i -th image, while $\alpha_i(x, y)$ is the value of α -matte for the corresponding pixel which acts as the weight. These weights $\alpha_i(x, y)$, should satisfy the following properties:

- 1) Total sum of all the weights for any given pixel should be equal to 1, i.e., $\sum_{i=1}^N \alpha_i(x, y) = 1 \quad \forall(x, y)$.
- 2) The weights should be non-negative, i.e., $\alpha_i(x, y) \geq 0 \quad \forall(x, y)$.

The image pixels are assumed to be normalized such that, $0 \leq u_i(x, y) \leq 1 \quad \forall(x, y)$.

The fusion of multi-exposure LDR images is intended for either a human observation or machine vision. Both of these objectives demand a high quality final image having high values of contrast and sharpness. A fused image should appear visually appealing to the human observers, and at the same time, the fused image should have a high amount of details, selectively chosen from the input data. This enhancement not only facilitates improved detail, but also aids other post-fusion vision operations such as segmentation.

The fused image is to be obtained from a set of LDR images which together encompasses a large dynamic range. Since this total range is far beyond the actual range of the final image, the fusion algorithm has to map pixels at the extremes of the gray level range towards the central region of the gray values around 0.5 to prevent saturation due to under- or over-exposure. This range of gray values confines to the dynamic range of the display/printing device. Hence, one of our primary objectives is to calculate the weights in such a way, that the gray values of appropriate pixels in the fused image lie closer to the central gray level to avoid under and over exposedness in the scene. From an information theoretic point of view, this problem can be restated as the problem of entropy maximization. The maximum entropy (MENT) problem is well studied for various problems in image processing, especially image restoration and reconstruction [14]–[17]. Here we apply the MENT method in a very different way for the mapping of a high dynamic range of the scene to the low dynamic range of the device. We define an objective function to obtain a set of weights $\{\alpha_i(x, y)\}$ which will maximize the entropy of the fused image $v(x, y)$ as,

$$\epsilon_1(\alpha) = - \int_x \int_y v(x, y) \log \left(\frac{v(x, y)}{0.5e} \right) dx dy \quad (2)$$

The factor of $0.5e$ has been added to the log-term to obtain the trivial solution of the equation at 0.5. In the present context of entropy maximization problem, the entropy of an image is directly defined over the normalized pixel values. This should not be confused with the general definition of the image entropy as the average information based on its statistical distribution.

As the trivial solution of Eq.(2) is given by an output image $v(x, y) = 0.5 \quad \forall(x, y)$, the output image has a poor contrast. Therefore, the MENT objective alone is not enough to obtain a clear and sharper fused image. For an image fusion scheme, we need to add a complementary objective to the optimization

function that will maintain the balance between the entropy maximization and the contrast of the image.

The variance of an image is one of the measures of contrast in the image. For the fused image $v(x, y)$, the variance σ^2 is defined as:

$$\sigma^2 = \frac{1}{XY} \int_x \int_y (v(x, y) - m(v))^2 dx dy, \quad (3)$$

where $m(v)$ is the mean of the fused image. A high value of variance indicates an image with well spread values of intensities over the given range. Images with a small value of variance lack details, while a high variance image appears sharp and visually appealing. In order to accomplish the objective of sharp and high contrast images, we additionally incorporate the variance to our objective function.

$$\epsilon_2(\alpha) = \frac{1}{XY} \int_x \int_y \left(v(x, y) - \frac{\left(\int_x \int_y v(x, y) dx dy \right)}{XY} \right)^2 dx dy. \quad (4)$$

These two objectives are complementary in a way that the former condition “pulls” the far distinct pixels towards the gray level 1/2, and the later condition “pushes” the pixels away from the mean.

The minimization problem defined using both of the aforementioned objectives deals only with the pixels on an individual basis. The pixels within a given neighborhood are fused without taking into consideration the spatial correlation among the pixels within the same image. The image pixels usually exhibit a moderate to high amount of correlation with the neighborhood pixels. When the input images are smooth, one would naturally expect the corresponding weights also to be smooth, i.e., α_i should be smooth in the x and y directions. The smoothness objective can be written as,

$$\epsilon_3(\alpha) = \int_x \int_y \sum_{i=1}^N (\alpha_{ix}(x, y)^2 + \alpha_{iy}(x, y)^2) dx dy, \quad (5)$$

where subscripts in x and y denote differentiation in the respective directions.

From Eq.(2),(4), and (5), we formulate the objective function for an unconstrained minimization as-

$$J(\alpha) = -\epsilon_1(\alpha) - \lambda_c \epsilon_2(\alpha) + \lambda_s \epsilon_3(\alpha) \quad (6)$$

$$\text{subject to, } \alpha_i \geq 0 \text{ and } \sum_{i=1}^N \alpha_i = 1 \quad \forall(x, y), \quad (7)$$

where λ_c and λ_s are the regularization parameters that balance weighting given to the variance term, and the smoothness term as compared to the MENT objective, respectively.

B. Variational Solution

Among the two constraints on the weights [Eq.(6)], the former constraint can easily be incorporated into the cost function in the form of a Lagrangian multiplier. However, an addition of the positivity constraint of the weights converts

the problem into a computationally demanding constrained optimization problem. In order to provide a computationally simple solution while maintaining the positivity of the weights, we define the α weights as the square of an auxiliary variable w , i.e.,

$$\alpha_i(x, y) \triangleq w_i^2(x, y) \quad \forall(x, y),$$

and modify the cost function and the constraints in Eq.(6) appropriately in terms of w . In the case of the smoothness term, however, the smoothness in w_i which is a positive square root of w_i^2 implies smoothness in the actual weights w_i^2 . Therefore, we impose the smoothness in w_i as an explicit constraint which ensures smoothness in the fused image. It may be noted that the actual weights α_i are always non-negative, irrespective of the sign of w . The normalization constraint, however, should be explicitly added to ensure that for every pixel (x, y) , the sum of the weights should equal 1, i.e.,

$$\sum_{i=1}^N w_i^2(x, y) = 1. \quad (8)$$

Now we provide the solution to the optimization problem using the Euler-Lagrange method. For the sake of brevity and easy understanding, we adopt the vector notations as follows. Let $\mathbf{u}(x, y) \in \mathbb{R}^N$ denote a vector consisting of N observations at the location (x, y) across the image stack, then $\mathbf{w}^2(x, y) \in \mathbb{R}^N$ denotes the weight vector for the same location. This vector can be considered as the elementwise product (also known as *Hadamard product*) of the vector $\mathbf{w}(x, y) \in \mathbb{R}^N$ with itself. Mathematically, we can write this expression as:

$$\mathbf{w}_i^2(x, y) = \mathbf{w}_i(x, y) \mathbf{w}_i(x, y) = \mathbf{w}(x, y) \circ \mathbf{w}(x, y) \quad (9)$$

where \circ is an elementwise product operator. Using the vector notations, the pixel of the resultant fused image $v(x, y)$ can be represented in the form of a dot product of the data vector with the corresponding weight vector.

$$v(x, y) = \mathbf{u}(x, y) \cdot \mathbf{w}^2(x, y) = \mathbf{u}^T(x, y) \mathbf{w}^2(x, y). \quad (10)$$

The combination of Eq.(6) and (8), gives the cost functional as-

$$\begin{aligned} J(\mathbf{w}) = & \int_x \int_y \left\{ (\mathbf{u}^T \mathbf{w}^2) \log \left(\frac{\mathbf{u}^T \mathbf{w}^2}{0.5e} \right) \right. \\ & - \lambda_c \left(\mathbf{u}^T \mathbf{w}^2 - \frac{1}{XY} \left(\int_x \int_y \mathbf{u}^T \mathbf{w}^2 dx dy \right) \right)^2 \\ & \left. + \lambda_s (\|\mathbf{w}_x\|^2 + \|\mathbf{w}_y\|^2) + \mu (\mathbf{w}^T \mathbf{w} - 1) \right\} dx dy. \quad (11) \end{aligned}$$

Here λ_c and λ_s are the scalars that weight the relative importance of the variance and the smoothness objectives, respectively, while μ is the Lagrangian multiplier for the unity constraint. Also, the arguments x and y of the functions are omitted for the purpose of brevity ($\mathbf{u} \equiv \mathbf{u}(x, y)$, etc.). The solution of Eq.(11) is obtained using the Euler-Lagrange equation.



Figure 1: Images of the indoor data captured under different exposure settings. Data courtesy: CAVE Lab, Columbia University.

On simplification of the Euler equation of $J(\mathbf{w})$ we get,

$$\begin{aligned} & (\mathbf{u} \circ \mathbf{w})(1 + \log(\mathbf{u}^T \mathbf{w}^2) - \log(0.5e)) - 2\lambda_c (\mathbf{u}^T \mathbf{w}^2 \\ & - \frac{\int_x \int_y \mathbf{u}^T \mathbf{w}^2 dx dy}{XY}) (\mathbf{u} \circ \mathbf{w} - \frac{\int_x \int_y \mathbf{u} \circ \mathbf{w} dx dy}{XY}) \\ & - \lambda_s \nabla^2 \mathbf{w} + \mu \mathbf{w} = \mathbf{0}, \end{aligned} \quad (12)$$

where \circ is an elementwise product operator, and ∇^2 is the Laplacian operator. The RHS of the equation indicates a zero vector.

A discrete approximation of the Laplacian operator is given as-

$$\nabla^2 \mathbf{w}(x, y) \approx \frac{4}{\delta^2} (\bar{\mathbf{w}}(x, y) - \mathbf{w}(x, y)), \quad (13)$$

where $\bar{\mathbf{w}}(x, y)$ is the local average of the weight vectors in the x and y dimensions, and δ is the distance between adjacent pixels, trivially set to 1. The iterative solution for the weight vector \mathbf{w} is obtained by re-arrangement of the terms after discretization as:

$$\begin{aligned} \mathbf{w}_{(k+1)} = & \frac{1}{1 + \frac{\mu \delta^2}{4 \lambda_s}} \left\{ \bar{\mathbf{w}}_{(k)} - \frac{\delta^2}{4 \lambda_s} \left(\mathbf{u} \circ \mathbf{w}_{(k)} (1 + \log(\mathbf{u}^T \mathbf{w}_{(k)}^2) \right. \right. \\ & - \log(0.5e) - 2\lambda_c (\mathbf{u}^T \mathbf{w}_{(k)}^2 - \frac{\sum_x \sum_y \mathbf{u}^T \mathbf{w}_{(k)}^2}{XY})) \\ & \left. \left. + 2 \frac{\lambda_c}{XY} \left(\mathbf{u}^T \mathbf{w}_{(k)} - \frac{\sum_x \sum_y \mathbf{u}^T \mathbf{w}_{(k)}^2}{XY} \right) \sum_x \sum_y \mathbf{u} \circ \mathbf{w}_{(k)} \right) \right\} \end{aligned} \quad (14)$$

where k indicates index of the iteration. It can be observed that the scalar μ appears only as a part of a positive scaling factor. Since the purpose of μ is to enforce the unit length of the weight vector, we can avoid this scaling factor, and explicitly normalize the weight vector to satisfy the necessary

constraint [18]. We introduce an intermediate variable z to represent un-normalized weights. Since \mathbf{w}^2 represents the actual weights, the normalization should be carried out to ensure the condition in Eq.(8). The final solution is thus given as-

$$\begin{aligned} \mathbf{z}_{(k+1)} = & \bar{\mathbf{w}}_{(k)} - \frac{\delta^2}{4 \lambda_s} \left(\mathbf{u} \circ \mathbf{w}_{(k)} (1 + \log(\mathbf{u}^T \mathbf{w}_{(k)}^2) - \log(0.5e) \right. \\ & - 2\lambda_c (\mathbf{u}^T \mathbf{w}_{(k)}^2 - \frac{\sum_x \sum_y \mathbf{u}^T \mathbf{w}_{(k)}^2}{XY})) \\ & \left. + 2 \frac{\lambda_c}{XY} \left(\mathbf{u}^T \mathbf{w}_{(k)}^2 - \frac{\sum_x \sum_y \mathbf{u}^T \mathbf{w}_{(k)}^2}{XY} \right) \sum_x \sum_y \mathbf{u} \circ \mathbf{w}_{(k)} \right) \end{aligned} \quad (15)$$

$$\mathbf{w}_{(k+1)} = + \sqrt{\frac{\mathbf{z}_{(k+1)} \circ \mathbf{z}_{(k+1)}}{\mathbf{z}_{(k+1)}^T \mathbf{z}_{(k+1)}}}. \quad (16)$$

The resultant fused image is given by Eq.(1) where $\alpha_i(x, y) = w_i^2(x, y)$.

In the case of color images, we apply our algorithm separately on each color channel to obtain the fused RGB image.

III. EXPERIMENTAL RESULTS

We have tested the proposed algorithm on several real datasets to verify its suitability for the practical purposes. These datasets include indoor as well as outdoor scenes captured under different exposure settings. The selection of these regularization parameters largely depends on the nature of the images, where the value of λ_c should be selected to approximately balance the numerical value of the MENT objective. As a rule of thumb, we may set λ_s to be nearly equal to $0.1 \times \lambda_c$. The small value of λ_s is due to the fact that it serves as a relative weighting given to the smoothness term of the minimization functional. A higher value of λ_s reduces the

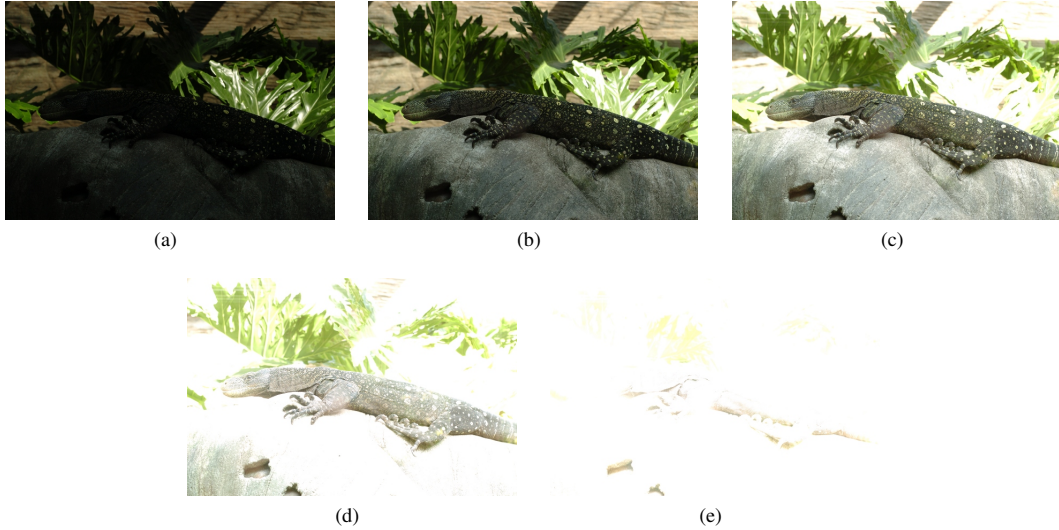


Figure 3: Images of the outdoor data captured under different exposure settings. Data courtesy: Eric Reinhard, University of Bristol.

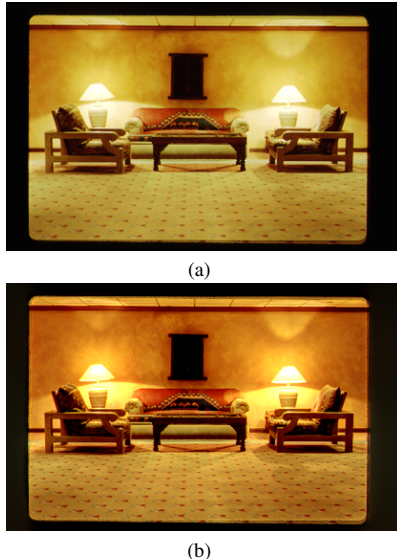


Figure 2: Resultant image from fusion of multi-exposure images in Fig.1 using (a) proposed approach, and (b) exposure fusion.

contrast in the image, as smoothness starts dominating over the others terms in the functional.

There are various techniques to stop an iterative minimization problem. We have followed a relative cost based criteria to conclude the iterative procedure. After every iteration k , we compute the cost of the functional $J_{(k)}$ using Eq.(11). The stopping rule is defined in terms of the relative difference in the cost function given by $\nabla J_{(k)} / J_{(k)}$. Typically we find the method to terminate after about 8-10 iterations.

We provide the experimental results on only three commonly used datasets for brevity. The first dataset depicts an

indoor scene (referred to as indoor data), the second dataset consists of multi-exposure LDR images of an outdoor scene, which is referred to as outdoor data. The third dataset consists of an indoor as well as an outdoor scene (referred to as mixed data). Figs.(1a - 1e) show 5 images of the same indoor scene under various exposures. It can easily be observed that different images highlight different features of the scene.

First two images, Fig.(1a) and (1b) highlight the texture and the shape of the lamps which are indistinguishable from light in other images. The images captured with a smaller exposure time [Fig.(1d-1e)] provide details of the texture of the chairs. Mid-exposure images provide various other details such as

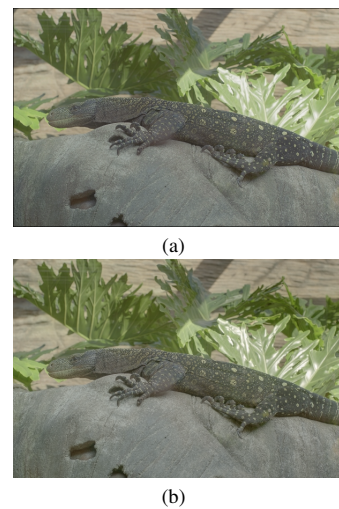


Figure 4: Resultant image from fusion of multi-exposure images in Fig.3 using (a) proposed approach, and (b) exposure fusion.

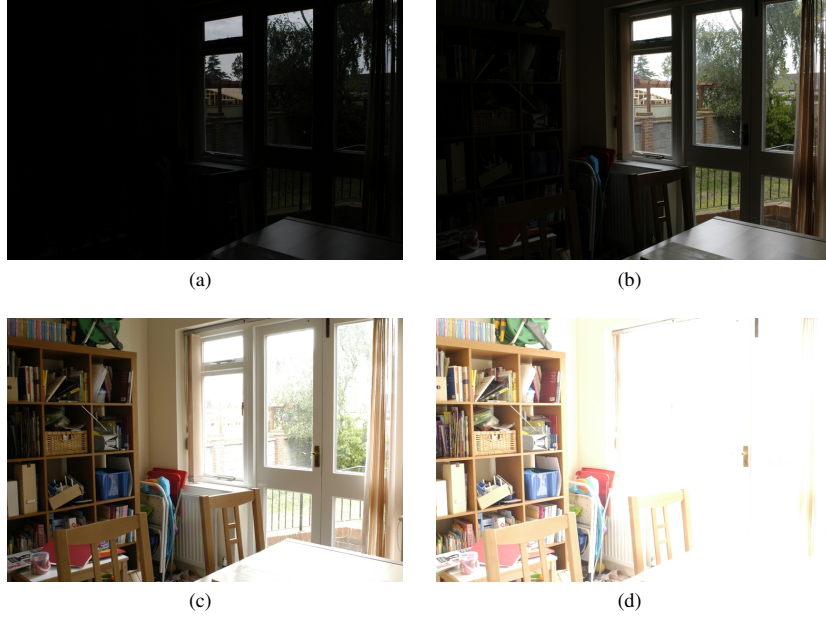


Figure 5: Images of the mixed data captured under different exposure settings. Data courtesy: Tom Mertens, Hasselt University.

shadows and the pattern on the wall, etc. The fusion of this scene using our approach is shown in Fig.(2a), which preserves all these details of the scene, without losing naturalness of the image. The fused image is able to preserve subtle details in the scene such as the structure of the wall, and the circular pattern on it formed due to the lights. The result of the exposure fusion technique [10] for the same dataset is shown in Fig.(2b) where we have selected equal weights for the contrast, saturation and exposedness as 1.0. Both the results are of very similar quality although the proposed method offers a better contrast (see Table I).

The outdoor test data includes a series of nine multiple exposure images of an outdoor scene which depicts a lizard and few leaves at the background. In the Figs.(3a-3e), we have shown only five representative images from the dataset. One can see the structure of leaves in some of the images, while the details of the lizard are apparent in images Figs.(3c-3d). Fig.(4a) shows the resultant fused image using the proposed approach. The resultant image has preserved several details from all the input LDR images such as- texture of the leaves, as well as of the background, without losing the details of the reptile. The resultant fused image for the same dataset using the exposure fusion technique is shown in Fig.(4b) for visual comparison.

The scene in the last dataset contains a set of LDR images of a mix of indoor and outdoor areas. Figs.(5a-5d) are the input multi-exposure images. The results of the proposed method and the exposure fusion method are shown in Fig.(6a), and Fig.(6b), respectively. The proposed method offers a much better contrast, compared to [10] as the corresponding result appears to be much over-exposed.

The fused image should possess a high amount of in-

formation content than the input LDR images. We may quantify the information richness of the image using its average information measure. This measure defined as $H = \sum_{i=0}^{L-1} -p_i \log(p_i)$, where p_i is the probability of having gray level i for an image with grayscale range $[0, L - 1]$ is commonly used for the evaluation of fusion methods. In the case of fusion of multi-exposure images for HDR creation,

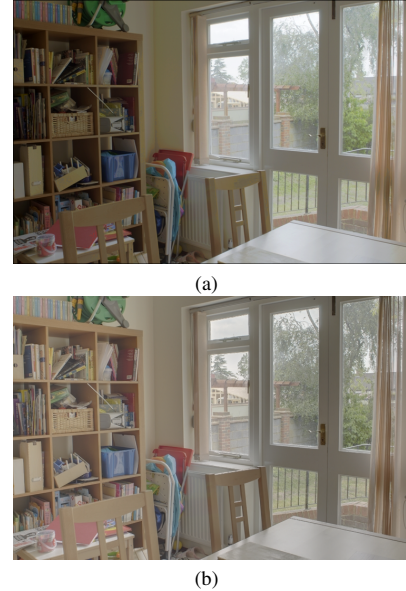


Figure 6: Resultant image from fusion of multi-exposure images in Fig.5 using (a) proposed approach, and (b) exposure fusion.

it has been used as evaluation criteria in [7]. In Table I, we provide the average information values of the resultant images generated using the proposed optimization-based technique. The measure for each of the color channel has been calculated separately, and the mean value is provided in the Table. Other than the first example, the proposed technique generates fused images with a significantly higher value than those produced by the exposure fusion technique. The variance of the fused image is also often considered as one of the quality parameters during the performance evaluation of the fusion techniques. It can be seen that the proposed technique yields fused images with a higher value of variance.

Table I: PERFORMANCE EVALUATION OF THE PROPOSED TECHNIQUE FOR 8-BIT DISPLAY.

Fusion Method	Variance			Avg. Information		
	Indoor	Outdoor	Mixed	Indoor	Outdoor	Mixed
Exposure Fusion	137.719	92.217	90.530	7.313	6.985	6.988
Proposed Method	145.863	96.719	96.388	7.324	7.117	7.431

IV. CONCLUSIONS

We have proposed an optimization-based technique for the fusion of multi-exposure images to generate an HDR-like image. This technique embeds the desired properties of the output image into the objective function, and provides an iterative solution to achieve the same. The proposed technique operates solely on the data, and does not require any knowledge of the camera response function, or the exposure settings. The fusion algorithm does not require any human intervention, except for the selection of the regularization parameters. We are currently working on selection of these parameters from the data statistic which will make the proposed scheme completely automatic. We are also investigating the possibilities of extending the applications to the fusion of multimodal data.

REFERENCES

- [1] E. Reinhard, G. Ward, S. Pattanaik, and P. Debevec, *High Dynamic Range Imaging: Acquisition, Display and Image-Based Lighting*. Morgan Kaufmann Publishers, December 2005.
- [2] T. Mitsunaga and S. Nayar, "Radiometric self calibration," in *IEEE Computer Society Conference on Computer Vision and Pattern Recognition*, vol. 1, pp. 2 vol. (xxiii+637+663), 1999.
- [3] P. E. Debevec and J. Malik, "Recovering high dynamic range radiance maps from photographs," in *Proceedings of the 24th annual conference on Computer graphics and interactive techniques*, SIGGRAPH '97, (New York, NY, USA), pp. 369–378, ACM Press/Addison-Wesley Publishing Co., 1997.
- [4] F. Drago, K. Myszkowski, T. Annen, and N. Chiba, "Adaptive logarithmic mapping for displaying high contrast scenes," *Computer Graphics Forum*, vol. 22, pp. 419–426, 2003.
- [5] R. Fattal, D. Lischinski, and M. Werman, "Gradient domain high dynamic range compression," *ACM Trans. Graph.*, vol. 21, pp. 249–256, July 2002.
- [6] Y. Li, L. Sharai, and E. H. Adelson, "Compressing and companding high dynamic range images with subband architectures," in *ACM SIGGRAPH 2005 Papers*, SIGGRAPH '05, (New York, NY, USA), pp. 836–844, ACM, 2005.
- [7] A. A. Goshtasby, "Fusion of multi-exposure images," *Image Vision Computing*, vol. 23, pp. 611–618, June 2005.
- [8] S. Raman and S. Chaudhuri, "Bilateral filter based compositing for variable exposure photography," in *Eurographics*, (Munich, Germany), 2009.
- [9] S. Raman and S. Chaudhuri, "A matte-less, variational approach to automatic scene compositing," in *IEEE 11th International Conference on Computer Vision*, (Rio De Janeiro, Brazil), pp. 1 – 6, Oct. 2007.
- [10] T. Mertens, J. Kautz, and F. Van Reeth, "Exposure fusion," in *15th Pacific Conference on Computer Graphics and Applications*, 2007, pp. 382 – 390, Nov. 2007.
- [11] O. Gallo, N. Gelfand, W.-C. Chen, M. Tico, and K. Pulli, "Artifact-free high dynamic range imaging," in *IEEE International Conference on Computational Photography*, pp. 1 – 7, Apr. 2009.
- [12] P.-Y. Lu, T.-H. Huang, M.-S. Wu, Y.-T. Cheng, and Y.-Y. Chuang, "High dynamic range image reconstruction from hand-held cameras," in *IEEE Conference on Computer Vision and Pattern Recognition*, pp. 509 – 516, Jun. 2009.
- [13] M. Tico, N. Gelfand, and K. Pulli, "Motion-blur-free exposure fusion," in *17th IEEE International Conference on Image Processing*, pp. 3321 – 3324, September 2010.
- [14] S. J. Wernecke and L. R. D'Addario, "Maximum entropy image reconstruction," *IEEE Trans. Comput.*, vol. 26, pp. 351–364, Apr. 1977.
- [15] S. F. Burch, S. F. Gull, and J. Skilling, "Image restoration by a powerful maximum entropy method," *Computer Vision, Graphics, and Image Processing*, vol. 23, no. 2, pp. 113 – 128, 1983.
- [16] S. Gull and J. Skilling, "Maximum entropy method in image processing," *IEE Proceedings of Communications, Radar and Signal Processing*, vol. 131, pp. 646 – 659, Oct. 1984.
- [17] E. S. Meinel, "Maximum-entropy image restoration: Lagrange and recursive techniques," *Journal Optical Society of America*, vol. 5, pp. 25–29, Jan. 1988.
- [18] M. J. Brooks and B. K. P. Horn, eds., *Shape from shading*. Cambridge, MA, USA: MIT Press, 1989.